View metadata, citation and similar papers at core.ac.uk
brought to you by CORE
provided by Electronic Sumy State University Institutional Repository

PROCEEDINGS OF THE INTERNATIONAL CONFERENCE NANOMATERIALS: APPLICATIONS AND PROPERTIES
Vol. **2** No 1, 01NTF29 (4pp) (2013)

Enhanced Luminescence of InGaN / GaN Vertical Light Emitting Diodes with an InGaN Protection Layer

N.D. Lam[1], S. Kim[1], J.J. Lee[1], K.R. Choi[2], M.H. Doan[3], H. Lim[3,*]

[1] *Department of Electrical and Computer Engineering, Ajou University, Suwon 443-749, Korea*
[2] *Division of Energy Systems Research, Ajou University, Suwon 443-749, Korea*
[3] *Center for Integrated Nanostructure Physics, Institute for Basic Science, Sungkyunkwan University (SKKU), Suwon 440-746, Korea*

(Received 10 June 2013; revised manuscript received 26 July 2013; published online 31 August 2013)

We have investigated the effectiveness of a thin n-$In_{0.2}Ga_{0.8}N$ layer inserted in the bottom n-GaN layer of InGaN/GaN blue light emitting diodes (LEDs) for the protection of multiple quantum wells during the laser lift-off process for vertical LED fabrication. The photoluminescence properties of the InGaN/GaN lateral LEDs are nearly identical irrespective of the existence of the n-$In_{0.2}Ga_{0.8}N$ insertion layer in the bottom n-GaN layer. However, such an insertion is found to effectively increase the photoluminescence intensity of the multiple quantum well and the carrier lifetime of the vertical LEDs. These improvements are attributed to the reduced defect generations in the vertical LEDs during the laser lift-off process due to the presence of the protection layer.

Keywords: GaN, InGaN, LEDs, Laser lift-off, Recombination enhanced defect reaction.

PACS numbers: 61.72.uj, 61.80.Ba

1. INTRODUCTION

The developments of GaN-based high brightness light emitting diodes (LEDs) have opened up the era of general solid-sate lightings [1, 2]. For such LEDs, high enough current injection and easy heat dissipation capabilities are needed to enable high power handling [3, 4]. GaN-based LEDs are usually grown on sapphire substrates, and the Ohmic contacts for n- and p-GaN are located laterally because of the existence of sapphire substrate. However, this lateral structure has limited current handling capacity and poor heat dissipation property [5]. To overcome such drawbacks, GaN-based vertical LED (VLED) structure has been developed. To make VLED, sapphire substrate is usually removed using a laser lift-off (LLO) technique after the LED structure is transferred to a metallic or Si substrate, and then n- and p-contacts are made for the vertical current injection [6]. Even though VLED exhibits a substantially improved capability to handle high current density [5, 6], they usually suffer from various problems caused by the defect formations during the LLO process [7, 8]. We have reported that, when the bottom GaN layer of the VLED is about 5 μm, as commonly adopted, defect formation is not confined to the bottom n-GaN layer but is extended even to the quantum well (QW) active region. We have also argued that the defect formation is mainly due to an athermal defect reaction, the so-called recombination enhanced defect reactions (REDRs) [8]. On the other hand, light output power is reported to increase with a decreasing n-GaN thickness in the VLEDs, the fact which might be attributed to the reduction of damaged n-GaN layer thickness [9].

Since the REDR process is induced by the absorption of photons employed during the LLO process, a way of improving the luminescence properties of the VLED would be masking the active region of the VLED from the laser beam. In this letter, we demonstrate that insertion of a thin $In_{0.2}Ga_{0.8}N$ layer in the bottom n-GaN layer effectively reduces the detrimental effect of KrF laser on the QW regions and, in turn, improves the luminescence properties of the InGaN/GaN VLED.

2. EXPERIMENTAL PROCEDURE

The details of the growth process, structure of the InGaN/GaN blue LEDs, and the LLO process employed in this study have been described elsewhere [8]. A lateral blue LED (sample type A) consists of a p-GaN/MQWs/4-μm-thick n-GaN/1-μm-thick undoped GaN/30-nm-thick GaN nucleation layer, from top to bottom, on a sapphire substrate. The structural parameters and growth conditions of the sample type B were identical with those of type A except that a 20-nm-thick Si-doped n-In0.2Ga0.8N protection layer was inserted in the n-GaN layer, keeping the total thickness of the n-layer constant of 4 μm. The thickness and In content of the protection layer were designed to be below the critical thickness and transparent to the luminescence emitted from the InGaN/GaN MQWs of the LEDs [10]. The thickness of the GaN layer below the MQW was intentionally taken as 5 μm since we wanted to discuss the influence of LLO process in a most commonly adopted InGaN/GaN LED structure. These LED structures were transferred to Cu substrates and then LLO process was performed employing a KrF laser with 544 mJ/cm^2 fluence, which slightly exceeds the threshold fluence of the LLO process [6, 8]. Crystal quality and structural properties of the samples were examined by high-resolution X-ray diffraction (HRXRD) and high-resolution transmission electron microscopy (HRTEM) observations. Luminescence properties of the lateral and vertical LEDs were investigated by a conventional

* hanjolim@ajou.ac.kr

 © 2013 Sumy State University

photoluminescence (PL) system (RPM2000, Accent) equipped with a 266-nm Nd:YAG laser and time-resolved photoluminescence (TRPL) measurements using a passively mode-locked Ti:sapphire laser operating at 836 nm at a repetition rate of 80 MHz. The femtosecond pulse was tripled to serve as the excitation source at a wavelength of 278 nm.

3. RESULTS AND DISCUSSION

Figures 1(a) and 1(b) show HRXRD spectra of the lateral LEDs without and with an n-$In_{0.2}Ga_{0.8}N$ protection layer, respectively. It is clear that the position and intensity of the diffraction peaks are almost identical for the two samples except for a broad shoulder around 33.9° due to an $In_{0.2}Ga_{0.8}N$ protection layer in sample B. For both A and B samples, the highest peak at about 34.5° is due to the GaN layer while the satellite "+1", "0", "-1", "-2", "-3" order peaks are due to the MQWs [11].

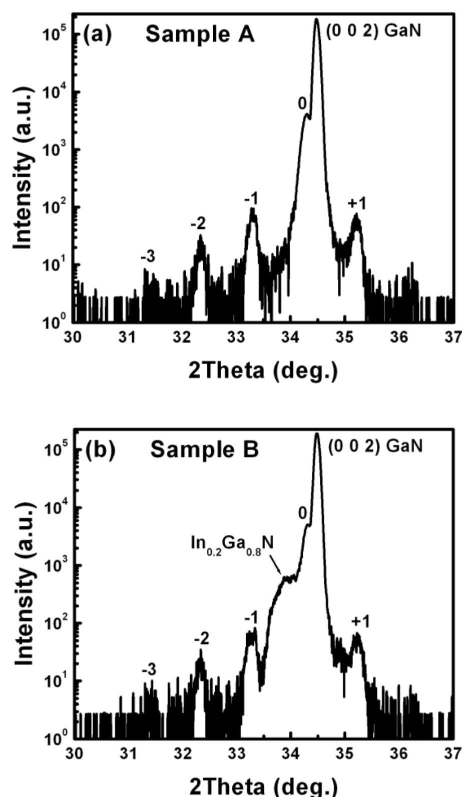

Fig. 1 - HRXRD spectra of the lateral LEDs (a) without and (b) with the InGaN protection layer

The fact that we can clearly observe these satellite peaks indicates that crystal and interface qualities of studied LEDs are good in both samples. From the X-ray diffraction spectrum, the In content of the InGaN protection layer is calculated to be 19.7% [11], which is close to the designed value of 20%. Cross-sectional HRTEM images of the LEDs also showed the existence of sharp interfaces in the InGaN/GaN MQWs and a 22 nm-thick n-InGaN protection layer at about 50 nm below the QWs in sample B (not shown here).

Figures 2(a) and 2(b) show room-temperature (RT) PL spectra of the lateral and vertical LED, respectyvly.

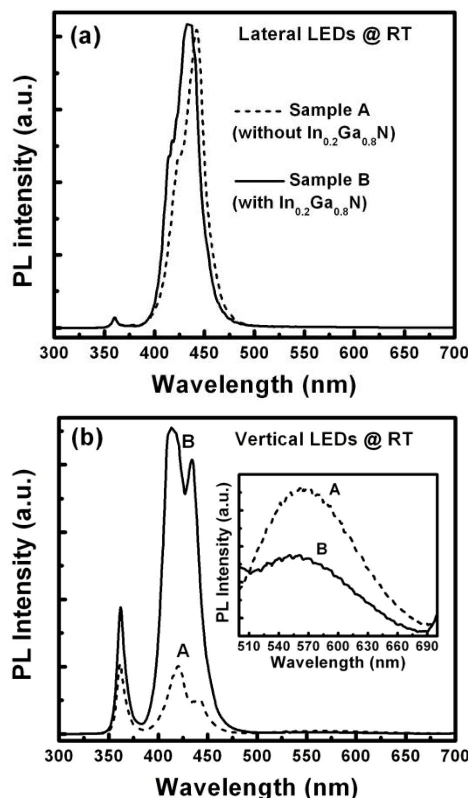

Fig. 2 - Room temperature PL spectra of the LEDs with and without n-$In_{0.2}Ga_{0.8}N$ protection layer (a) on the sapphire substrates and (b) on the Cu substrates after the LLO process. The inset in Fig. 2(b) shows magnified yellow emission regions

The blue (UV) emission peak around 440(360) nm in Fig. 2(a) comes from the InGaN/GaN MQWs (GaN layer). Slight differences in the blue PL peak position and intensity between sample A and B may be due to the variations of the homogeneity. The shoulders at about 417 and 423 nm have been related to the various mechanisms such as insufficient In incorporation in QWs [12], reduced well width [13], and reduced strain or polarization [14]. In the PL spectra of the VLEDs [Fig. 2(b)], the ratio of integrated QW PL intensity for sample B to that for sample A is found to be greater than four, while the "yellow" emission which is related to the defects [15, 16] shows an opposite trend. We have shown that the decrease (increase) of QW (yellow) emission is mainly due to the increase of defects in the QWs (n-GaN layer) generated most likely by the REDRs induced by the absorption of 5 eV KrF photons during the LLO process [8]. Therefore, these improvements in the VLEDs through the adoption of the protection layer are clearly attributed to the reduced propagation of KrF photons into the MQWs and the n-GaN layers. The number of KrF photons arriving at the first QW (counted from the sapphire substrate side) is calculated to be ~$1.5 \cdot 10^{16}$ cm^{-2} when the protection layer is absent [8]. The number of KrF photons arriving at the MQWs due to the insertion of the 20 nm-thick $In_{0.2}Ga_{0.8}N$ protection layer is estimated by calculating the reflection and transmission of an electromagnetic wave in the GaN/$In_{0.2}Ga_{0.8}N$/GaN layer system as a function of the

$In_{0.2}Ga_{0.8}N$ thickness. In this calculation, refractive indices of the GaN and $In_{0.2}Ga_{0.8}N$ measured by an ellipsometry technique at the wavelength of 248 nm (n_{GaN} = 2.46 + 0.33i and n_{InGaN} = 1.47 + 0.68i) are used. Fabry-Perot interference was not observed in the simulation due to the high loss of GaN, and a 20-nm-thick $In_{0.2}Ga_{0.8}N$ layer showed about 54% transmission. This reduction of photon number arriving at the MQWs significantly decreases the defect generation by the REDRs in the MQWs and, in turn, improves the luminescence properties of the InGaN/GaN VLED.

Figures 3(a) and 3(b) show cross-sectional HRTEM images of MQW regions in the VLEDs for the samples A and B, respectively. It can be seen that the VLED fabricated without the protection layer (A) reveals intermixed QW regions, while the VLED fabricated with the protection layer (B) shows well-defined sharper interfaces. Therefore, the observed severe degradation of the MQW luminescence from the VLED without the protection layer [Fig. 2(b)] should be attributed to the micro-defects generated during the QW intermixing by REDRs. Note that PL spectra of the VLEDs in Fig. 2(b) show well separated high and low energy components in the QW emissions, and the high energy emission peak is dominant especially in the spectrum of VLED without the protection layer. It is also interesting to note that the QW emissions of the fabricated VLEDs in Fig. 2(b) show a slight blue-shift compared to those of the lateral LEDs in Fig. 2(a).

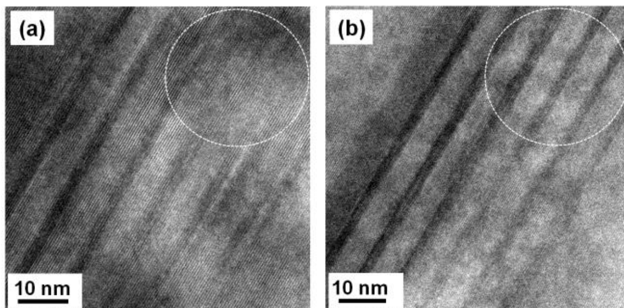

Fig. 3 - Cross-sectional HRTEM images of the sample (a) A (without protection layer) and (b) B (with protection layer) after the LLO process. QW intermixing is more apparent in sample A (as can be seen in the circle-marked region)

Such dominancy of high energy component and blue-shift of the QW emissions in the VLEDs should be attributed to the QW intermixing. Note that this argument means that QWs may be intermixed to a certain extent even with the KrF photon flux of $\sim 5 \cdot 10^{15} cm^{-2}$. This phenomenon may be explained by the fact that absorption of one KrF photon will induce about 10^2 phonon generations, in addition to REDRs, and, in turn, the REDRs process might be facilitated by such atomic vibrations as we have discussed in our previous report [8].

A more direct evidence of the fact that the defect generation during the QW intermixing process is the main cause of the degradation of the MQW emission in the VLED is sought by measuring the carrier lifetimes in the VLEDs. Figure 4 shows the RT TRPL spectra of the LEDs with and without the protection layer before and after the LLO process, respectively. One sees that

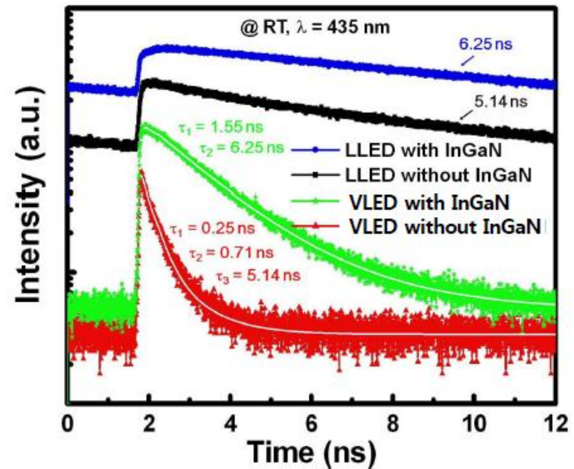

Fig. 4 - Room temperature time-resolved PL spectra for the QW emissions of samples A and B before (LLED) and after (VLED) the LLO process. The white curves in the TRPL spectra of the LLO-processed samples are the fitted curves

the RT PL decay times of the lateral LEDs, which are about 5~6 ns and well consistent with the one reported in the literature [17], are much longer than those of the vertical LEDs. The measured decay time τ_M is related to the radiative decay time τ_R and nonradiative decay time τ_{NR} as $1/\tau_M = 1/\tau_R + 1/\tau_{NR}$. This indicates that nonradiative defects are generated in the QWs through the LLO process even in the VLED with the protection layer. The decay kinetics of the VLED without the protection layer could be fitted well only with the three decay constants, while the VLED with the protection layer was fitted well with two decay constants model. Thus more complex defects, perhaps dislocation loops [8], are believed to be created in the VLED without the protection layer, as the number of KrF photons impinging to the MQWs is larger in the VLED without the protection layer.

It is evident that the adoption of a thin InGaN protection layer apparently improves the optical properties of the MQWs in the InGaN/GaN VLEDs. From a study on the dependence of protection efficiency on the In composition and thickness of the protection layer (not shown here), we found that protection efficiency generally increases as In content and thickness are increased up to certain critical values. In this respect, further study is needed to design an optimum protection structure which may completely block the propagation of KrF
photons into the MQWs and result in highly enhanced emission efficiency.

4. CONCLUSION

In summary, we have performed the PL and TRPL experiments and HRTEM observations to investigate the effectiveness of a 20-nm-thick $In_{0.2}Ga_{0.8}N$ layer which is designed to protect the MQWs of the InGaN/GaN LEDs during the LLO process. All the optical experimental results show that the luminescence properties of the MQWs in the VLEDs with the protection layer are much better than those of the VLEDs without the protection layer. HRTEM

observations reveal that this improvement of luminescence properties is based on the reduction of the QW intermixing, which is believed to be induced by REDR, through the decrease of transmitted KrF photons to the MQWs.

AKNOWLEDGMENTS

This work is supported by the National Research Foundation Grants (Mid-career Researcher Program: 2009-0083803 and KRF-2007-331-D00250). This work is also supported by the Ajou University research fellowship of 2009.

REFERENCES

1. D.A. Steigerwald, J.C. Bhat, D. Collins, R.M. Fletcher, M.O. Holcomb, M.J. Ludowise, P.S. Martin, S.L. Rudaz, *IEEE J. Sel. Top. Quan. Electron.* **8**, 310 (2002).
2. S. Nakamura, *MRS Bulletin.* **34**, 101 (2009).
3. M.H. Crawford, *IEEE J. Sel. Top. Quan. Electron.* **15**, 1028 (2009).
4. A. Laubsch, M. Sabathil, J. Baur, M. Peter, and B. Hahn, *IEEE Tran. Electron. Dev.* **57**, 79 (2010).
5. C.-F. Chu, C.-C. Cheng, W.-H. Liu, J.-Y. Chu, F.-H. Fan, H.-C. Cheng, T. Doan, C.A. Tran, *Proc. IEEE.* **98**, 1197 (2010).
6. C.-F. Chu, F.-I. Lai, J.-T. Chu, C.-C. Yu, C.-F. Lin, H.-C. Kuo, S.C. Wang, *J. Appl. Phys.* **95**, 3916 (2004).
7. W.H. Chen, X.N. Kang, X.D. Hu, R. Lee, Y.J. Wang, T.J. Yu, Z.J. Yang, G.Y. Zhang, L. Shan, K.X. Liu, X.D. Shan, L.P. You, D.P. Yu, *Appl. Phys. Lett.* **91**, 121114 (2007).
8. M.H. Doan, S. Kim, J.J. Lee, H. Lim, F. Rotermund, K. Kim, *AIP Advances.* **2**, 022122 (2012).
9. H.H. Jeong, S.Y. Lee, K.K. Choi, J.-O. Song, J.-H. Lee, T.-Y. Song, *Microelectron. Eng.* **88**, 3164 (2011).
10. F.K. Yam, Z. Hassan, *Superlattices and Microstructures* **43**, 1 (2008).
11. M.E. Vickers, M.J. Kappers, T.M. Smeeton, E.J. Thrush, J.S. Barnard, C.J. Humphreys, *J. Appl. Phys.* **94**, 1565 (2003).
12. F. Hizel, G. Klewer, S. Lahmann, U. Rossow, A. Hangleiter, *Phys. Rev. B* **72**, 081309(R) (2005).
13. A. Hangleiter, F. Hitzel, C. Netzel, D. Fuhrmann, U. Rossow, G. Ade, P. Hinze, *Phys. Rev. Lett.* **95**, 127402 (2005).
14. C.L. Yang, L. Ding, J.N. Wang, K.K. Fung, W.K. Ge, H. Liang, L.S. Yu, Y.D. Qi, D.L. Wang, Z.D. Lu, K.M. Lau, *J. Appl. Phys.* **98**, 023703 (2005).
15. J. Neugebaner and C.G. Van de Walle, *Appl. Phys. Lett.* **69**, 503 (1996).
16. M.A. Reshchikow, H. Morkoc, *J. Appl. Phys.* **97**, 061301 (2005).
17. Y.-H. Cho, G.H. Gainer, A.J. Fischer, J.J. Song, S. Keller, U.K. Mishra, S.P. DenBaars, *Appl. Phys. Lett.* **73**, 1370 (1998).